Biophysical Chemistry, 38 (1990) 167–178
Elsevier

BIOCHE 01517

Model anionic polysaccharide matrices exhibit lower charge selectivity than is normally associated with kidney ultrafiltration

Oliver Zamparo and Wayne D. Comper

Department of Biochemistry, Monash University, Clayton, Vic. 3168, Australia

Received 26 March 1990
Revised manuscript received 30 May 1990
Accepted 26 June 1990

The influence of the anionic polysaccharide matrix (APM) of the glomerular basement membrane (GBM) on water transport and macromolecular transport charge selectivity has been studied in model systems which enable the analysis of the specific properties of the APM. Various APMs were studied including heparin and heparin-like polysaccharides, chondroitin sulfate and dextran sulfate. Upper estimates of the APM concentration in the GBM were obtained by relating measurements of the specific hydraulic conductivity of the heparin-like polysaccharides to measurements of single nephron glomerular filtration rate. This gave values of 40–45 mg ml^{-1} of polysaccharide, which was then used to analyse factors contributing to macromolecular charge selectivity. Transport analysis of the test dextran probes, used for previous in vivo clearance studies, in APMs demonstrated that there were no differential charge effects at APM concentrations in the range predicted above in the GBM. This was also found to be the case for the partitioning of anionic test probes at the APM-solution interface as measured directly using frontal gel chromatography and through thermodynamic analysis of sedimentation and diffusion data. These studies demonstrated that previous biophysical interpretations of glomerular charge selectivity have severely overestimated the partitioning effect due to the electrostatic effects of polyion-polyion interaction.

1. Introduction

Studies of the fractional clearance of charged dextran transport probes relative to inulin in kidneys have demonstrated that, apart from size selectivity, the kidney exhibits charge selectivity. For a given hydrodynamic size, negatively charged dextran (dextran sulfate) shows a lower clearance as compared to its uncharged counterpart, dextran [5,6], whereas positively charged dextran (diethylaminoethyl (DEAE) dextran) shows higher clearance relative to dextran [3]. The functional significance of this charge selectivity is not clear but it does represent a characteristic of normal kidney ultrafiltration. The relative clearance of dextran sulfate vs dextran has been demonstrated to be considerably less in proteinuric states, derived either from nephrotoxic serum nephritis [1] or the administration of puromycin aminonucleoside to rats [4]. These proteinurias have been correlated with a loss of fixed negative charge from the glomerular basement membrane (GBM). Increased glomerular permeability to albumin has also been shown following specific enzyme digestion of heparan sulfate in the GBM [24].

The theoretical, biophysical interpretation of renal charge selectivity by Deen et al. [12] has been based on the fact that transglomerular macromolecular transport occurs as a passive process in the intercellular space of the capillary wall and across the GBM. The fixed negative charges of the basement membrane, which are mainly contrib-

Correspondence address: W.D. Comper, Department of Biochemistry, Monash University, Clayton, Vic. 3168, Australia.

uted by the ionizable groups of extracellular heparan sulfate proteoglycan and to a lesser extent by chondroitin sulfate proteoglycan [15], then singularly account for transport charge selectivity. Quantitative prediction of macromolecular charge selectivity was possible utilizing the classical Nernst-Planck equations. Charge selectivity was primarily derived from the Donnan equilibrium that governs the partition of charged macromolecules at the membrane-solution interfaces. It was predicted that with increasing molecular weight of the charged dextran and therefore increasing charge or total valence on the macromolecule, then the greater is the charge selectivity. Their predictions gave a value of fixed charge concentration (assumed uniform throughout the GBM) of 165 mequiv. l^{-1}.

While charge selectivity has been demonstrated in films of isolated basement membranes [2], its degree is considerably lower than that observed in in vivo fractional clearance studies. There is now growing evidence too that suggests that some of the assumptions associated with the biophysical interpretation are inappropriate. The GBM heparan sulfate proteoglycans are recognized as being nonuniformly distributed and appear concentrated in the laminae rarae interna and externa regions [16,27]. Further, the GBM concentration of heparan sulfate has been subject to widely varying estimates. The fixed charge concentration of 165 mequiv. l^{-1} of Deen et al. [12] would translate to 40–45 mg ml^{-1} of heparan sulfate, which compares to the much lower values of 26.5 mequiv. l^{-1} from sodium chloride distribution across the GBM [36] and of 30 μg heparan sulfate ml^{-1} (basement membrane) as determined by chemical analysis [26]. We also envisage a serious problem using the Nernst-Planck equations associated with the applicability of the classical Donnan equilibrium between a charged membrane and permeant macromolecules of multiple valence [12]. This has yet to be experimentally verified, and further, the Donnan equilibrium tacitly assumes that the mobile component is a point source as distinct from the relatively large hydrodynamic volume occupied by the charged dextran probes. Another dilemma associated with transglomerular transport is whether it proceeds purely by passive extracellular mechanisms as morphological evidence would suggest the involvement of cell-mediated processes [22].

In this study the role of the anionic polysaccharide matrix (APM) of the GBM is examined in relation to the partition of permeant material at the membrane-solution interface and transport within the membrane. No theoretical assumptions are made, but rather we test the hypothesis that the passive anionic polysaccharide matrix gives rise to the charge selectivity associated with kidney ultrafiltration. Studies are made on similar charged dextran test probes that have been used previously in in vivo clearance studies. To examine whether passive, physical processes could account for glomerular charge selectivity we use a model system of concentrated polyanionic polysaccharide as representative of the APM in the GBM. Actual charge selectivity of the GBM, when rationalised on the basis of the biophysical Nernst-Planck model, can be delineated into two processes, namely, (1) the ability of the test molecule to enter the membrane-matrix, and (2) the rate at which the test molecule is transported within the membrane. Both these processes will be experimentally studied independently in the model system. The analysis of the partitioning of the test dextran probes at the APM-solution interface is performed by frontal gel chromatography [33]. Quantitative estimates of polyion-polyion interactions that constitute Donnan partitioning are also made through the analysis of thermodynamic nonideality of various polysaccharide preparations including heparin and dextran sulfate as obtained by sedimentation-diffusion analysis in the ultracentrifuge [9,37]. Transport measurements of the test dextran probes in APM are carried out in diffusion cells [28] which create a shear formed liquid-liquid boundary. The two major types of APM that have been used in this part of the investigation are concentrated solutions of high molecular weight dextran sulfate and chondroitin sulfate. We regard the use of dextran sulfate with its high charge density (2.01 ionizable groups per hexose residue [35]) as being a particularly suitable APM to test the effects of polysaccharide anionic charge on transport and partitioning of mobile charged solutes.

2. Theory

2.1. The Nernst-Planck model

The concentration profiles associated with the transport of molecules across a passive, anionic charged membrane are schematically shown in fig. 1. There are three regions of importance in the Nernst-Planck model governing transport. Uncharged mobile solutes will undergo partitioning at the two membrane-solution interfaces (due to steric hindrance). Their transport within the membrane will generate a concentration gradient dependent on membrane thickness and the dynamic interaction of the mobile solute with the membrane. Charge selectivity associated with anionic and cationic mobile solutes will be associated with differential effects at these three regions. For simplicity we will assume that, for transport left to right in fig. 1, the charge selectivity is governed primarily by the initial partitioning at the membrane-solution interface and transport within the membrane. It is assumed that the second partition will not affect selectivity to any significant extent. This approach will tend to overestimate the degree of charge selectivity offered by the membrane.

2.2. Component nomenclature

The permeant species through the APM is designated as component 1, the APM as component 2, and solvent (water plus NaCl) as component 3. The component designations are for the electroneutral components only. The electroneutral simple electrolyte, normally NaCl, when considered specifically is designated as component s.

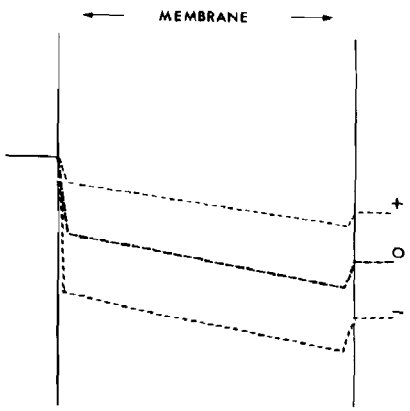

Fig. 1. Schematic diagram of concentration profiles of charged and uncharged permeant species across a negatively charged membrane. The concentration gradient extends from left to right across the membrane.

2.3. Hydraulic conductivity and osmotic pressure

The use of the sedimentation-diffusion technique in the ultracentrifuge provides a powerful tool to evaluate specific hydraulic conductivity and thermodynamic nonideality. The rationale behind using these parameters is that (1) the hydraulic conductivity can be used to evaluate maximal APM concentration in the GBM using measurements of single nephron GFR and (2) the thermodynamic nonideality can be used to estimate, not only osmotic pressure but also partition coefficients of permeant species at the APM-external solution interface. The latter estimate will provide information on the role of APM in the GBM in conferring charge selectivity on test probes at the GBM-solution interface.

Irreversible thermodynamics provides an expression for solute flux (J_i) associated with sedimentation in a volume fixed frame of reference [14],

$$J_i = (S_i)_v C_i \omega^2 r - (D_i)_v (\partial C_i/\partial r) \quad (i = 1, 2) \qquad (1)$$

where ω is the angular speed of the rotor (rad per s), r the distance from the center of the rotor, $(S_i)_v$ the sedimentation coefficient and $(D_i)_v$ the mutual diffusion coefficient of solute i in a volume fixed frame of reference, and C_i the concentration of i in mass/volume units. Expressions for $(S_i)_v$ and $(D_i)_v$ have been derived previously [9] such that

$$(S_i)_v = (1 - \rho v_i)(1 - \phi_i) M_i/f_{i3} \qquad (2)$$

and

$$(D_i)_v = (1 - \phi_i)^2 (M_i/f_{i3})(\partial \Pi^*/\partial C_i)_{T,\mu_3} \qquad (3)$$

Substituting eqs 2 and 3 into eq. 1 gives

$$J_i = (1 - \phi_i)(M_i/f_{i3})\left[C_i \omega^2 (1 - \rho v_i) \times \left\{(\partial r^2/2)/\partial r\right\} - (1 - \phi_i)(\partial \Pi^*/\partial r)_{T,\mu_3}\right] \qquad (4)$$

where ρ is the solution density, v_i the partial specific volume of i, ϕ_i the volume fraction of i, M_i the molecular weight of i, f_{i3} the hydrodynamic frictional coefficient which represents the frictional interaction between solute and solvent, Π^* the osmotic pressure, T the temperature and μ_3 the chemical potential of solvent. This equation then represents a balance of a mechanical force ($C_i\omega^2(1-\rho v_i)\partial r^2/2$) and an osmotic force ($(1-\phi_t)\partial\Pi^*$) on the solute. The equation bears a marked resemblance to D'Arcy's law where the coefficient of eq. 4 is directly related to the effective diffusion coefficient of component i ($= RT/f_{i3}$ where R is the universal gas constant) which governs the kinetics of both pressure-driven processes, namely, hydraulic flow and osmosis. At high rotor speeds the flux J_i is determined primarily by the sedimentation coefficient. A direct relationship between specific hydraulic conductivity, k_i, and the sedimentation coefficient has been derived [21]

$$k_i = \eta_3(S_i)_v/C_i(1-(v_i/v_3)) \tag{5}$$

where η_3 is the viscosity of solvent.

At lower rotor speeds, where sedimentation is negligible, the mutual diffusion coefficient of the solute may be evaluated. The combination of both the D_i and S_i data may then be used to calculate the thermodynamic nonideality term

$$(\partial\Pi^*/\partial C_i)_{T,\mu_3} = (1-\rho v_i)D_i/(1-\phi_i)S_i \tag{6}$$

This equation is important for two reasons. Firstly, integration of eq. 6 with respect to C_i yields osmotic pressure as a function of C_i. Secondly, the $(\partial\Pi^*/\partial C_i)$ term may be used to evaluate partition coefficients, at the APM-solution interfaces, as described in section 2.4.

Most experiments are performed with macromolecular solutes in thermodynamic equilibrium with physiological saline. Under these conditions for polyelectrolytes the equation for the mutual diffusion coefficient takes on the same form as eq. 3 [34]. The equation for the sedimentation coefficient of polyelectrolytes is also the same as that described by eq. 2 as simple salt effects on $(S_i)_v$ (or electrolyte dissipation) have been shown to be negligible for connective tissue polysaccharides [37].

2.4. The partitioning of a mobile component between the APM and the external solution

The chemical potentials of the permeating species in the APM region (designated by $''$) and the external solution (designated by $'$) are

$$\mu_1' = \mu_1^\Theta + RT\ \ln(y_1'C_1'/C^\Theta) \tag{7}$$

$$\mu_1'' = \mu_1^\Theta + RT\ \ln(y_1''C_1''/C^\Theta) \tag{8}$$

where μ_1 is the chemical potential of component 1, μ_1^Θ the standard chemical potential, C^Θ a standard value of mass concentration and y_1 the activity coefficient of 1. It is assumed that the pressure-volume terms in eqs 7 and 8 are negligible. At equilibrium

$$\mu_1' = \mu_1''$$

so that using eqs 7 and 8 we obtain for trace quantities of component 1

$$\ln K = -\ln\ y_1'' \ (\text{for } C_1 \to 0) \tag{9}$$

where the partition coefficient $K = C_1''/C_1'$. The partition coefficient, through eq. 8, is related to the thermodynamic nonideality term by the following at constant T, μ_3, and C_2 in $''$

$$(\partial\Pi^*/\partial C_1) = (C_1/M_1)(\partial\mu_1/\partial C_1) + (C_2/M_2)(\partial\mu_2/\partial C_1) \tag{10}$$

For simplicity we utilise equations that have neglected the influence of simple electrolyte (however, see below). A number of studies have now established that Π^* (or $\partial\Pi^*/\partial C$) for polysaccharides and proteoglycans is molecular weight independent in semidilute solutions [8–11,31]. For these systems we consider the special case that component 1 is chemically identical to component 2, and exhibits the same thermodynamic nonideality, but is different in that it is smaller than 2. Since the $(\partial\mu_i/\partial C_i)$ terms are molecular weight independent we can express eq. 10 in terms of $\ln K$ of eq. 9 such that [19]

$$(\partial\Pi^*/\partial C_1) = RT(1-\ln K)/M_1 \tag{11}$$

or

$$K = e^{-\{(M_1/RT)(\partial \Pi^*/\partial C_1)-1\}} \quad (12)$$

The factors then that will contribute to the partitioning of component 1 will be embodied in the osmotic pressure terms of mixtures of components 1 and 2. The osmotic pressure can be regarded as being the sum of the following parameters [8], namely,

$$\Pi^*_{\text{total}} = \Pi^*_{\text{counterion-polyion}} + \Pi^*_{\text{excluded volume}} \quad (13)$$

where

$$\Pi^*_{\text{excluded volume}} = \Pi^*_{\text{nonelectrostatic}} + \Pi^*_{\text{electrostatic}} \quad (14)$$

and where the $\Pi^*_{\text{counterion-polyion}}$ term represents the contribution of micro-counterion interaction and its associated simple electrolyte distribution to the osmotic pressure, i.e., the Donnan term. The $\Pi^*_{\text{excluded volume}}$ term is a function of polyion-polyion interactions which will have an entropic excluded volume component associated with the uncharged properties of the interacting polymers and an electrostatic component associated with the Coulombic charge-charge interactions. These electrostatic interactions may enhance excluded volume, as in the case of polyanion-APM interaction, or decrease excluded volume as in the case of polycation-APM interaction. It will be these types of electrostatic interactions that will determine charge selectivity at the partition of the APM-external solution interface.

The influence of simple electrolyte on the distribution of permanent electrolyte (being chemically identical to the APM) is expected to be small. At an interface, the Donnan equilibrium of components (with $c_1 \to 0$) can be approximated by the following expression

$$(z_1 c_1' + c_s')\, c_s' (y_s')^2 = (z_1 c_1'' + z_2 c_2'' + c_s'')\, c_s'' (y_s'')^2 \quad (15)$$

where z_i represents the effective degree of ionization of the polyion, c_i the molar concentration of i and y_s the activity coefficient of the simple electrolyte. For $c_1 \to 0$ and with the assumption that the activity coefficient of salt is the same in both phases (likely when $c_2'' \leq c_s'$) then eq. 15 reduces to

$$c_1''/c_1' \simeq c_s'/c_s'' \quad (16)$$

This equation suggests that the permeant polyion will distribute itself in a manner inversely proportional to simple electrolyte; even at high concentrations, i.e., 160 mequiv. l^{-1} the distribution of salt would not be expected to be greater than 1.5 [23,35].

3. Experimental

3.1. Materials

Heparin (porcine intestinal mucosa), chondroitin sulfate (bovine tracheal) and benzylated dialysis tubing (molecular weight cutoff $\simeq$ 2000) were purchased from Sigma (St. Louis, MO). Dextran sulfate T500 (weight average molecular weight (MW) of 500 000 according to manufacturer's specifications), dextran T500 (MW $\simeq$ 500 000), dextran T10, dextran sulfate T10, DEAE dextran T10 and Sephadex G-100 were from Pharmacia (Sweden). Sodium boro[^{3}H]hydride (spec. act. 131.2 mCi mg^{-1}) was from Amersham (U.K.). Controlled-pore glass with a mean pore diameter of 229 Å was from Electro-Nucleonics (Fairfield, NJ) (A240) and one with a mean pore diameter of 150 Å (CPG-120-120) was from Sigma. All other reagents used were of the highest grade commercially available.

3.2. Methods

3.2.1. Sedimentation and diffusion analysis

The sedimentation coefficients were measured in an analytical ultracentrifuge at a temperature of 20 °C by methods which have been described in detail elsewhere [10,11,37].

3.2.2. Tracer diffusion in APM

Tracer diffusion coefficients of ^{3}H-labelled test dextran probes (table 1) were measured in a diffusion cell [28,32] that consists of two cylindrical chambers that rotate to shear-form a sharp, free liquid boundary between upper and lower solutions. The labelled species was always placed initially in the lower chamber. The APM was in both chambers but with a 5 mg ml^{-1} gradient between the upper and lower solutions which was to ensure

Table 1

Physicochemical characteristics of test dextran probes

	Charge substitution (ionizable groups per disaccharide residue)	Diffusion coefficient at infinite dilution (D_0) ($cm^2\ s^{-1}$)	Radius [b] (Å)
[^{3}H]Dextran sulfate T10	4.02	1.6×10^{-7}	17
[^{3}H]DEAE Dextran T10 (i)	1.32 [a]	9.5×10^{-7}	25
[^{3}H]DEAE Dextran T10 (ii)	1.32 [a]	21.0×10^{-7}	13
[^{3}H]Dextran T10	0	10.5×10^{-7}	20

[a] According to manufacturer's specifications.

[b] Obtained by the estimation of K_{av} on Sephadex G-100 column (50 × 1.8 cm) and the relationship between K_{av} and the effective solute radius [7].

against gravitational instabilities that may form in multicomponent systems. For measurements of the diffusion coefficient without APM material sorbitol at 5 mg ml^{-1} was used in the lower chamber. All experiments were run in duplicate over four different time points and at a temperature of 23 ± 1°C.

3.2.3. Frontal gel chromatography

The partition coefficient between APM and mobile probe was evaluated by use of a technique described previously [33], where the interface between solutions at a pore in a gel (which excludes the APM) is equivalent to that at the interface of the solution and the APM. For an APM of dextran sulfate T500 a column (dimensions 52 × 1.8 cm) (void volume 21 ml and total volume 36 ml) was packed with controlled-pore glass (pore diameter 229 Å) (deaerated in the presence of polyethylene glycol), and 30 ml of a concentrated dextran sulfate solution containing ^{3}H-labelled mobile probe was then applied and run at a 4 ml h^{-1} flow rate with 1-ml fractions being collected. For an APM of chondroitin sulfate (bovine trachea), a column (dimensions 20 × 1.2 cm) with controlled-pore glass (pore diameter 150 Å) was run at 5 ml h^{-1}.

3.2.4. Tritium labelling

Tritiation of the dextrans and chondroitin sulfate was carried out as described by Van Damme et al. [32] using a reductive technique with sodium boro[^{3}H]hydride. The preparations were then fractionated on a Sephadex G-75 column with 80% of the major peak being pooled and used for transport experiments. Radioactive counting analysis of the tracer dextrans has also been described previously [32].

3.2.5. Preparation of solutions

To represent physiological ionic conditions, the polymers used in the biophysical measurements were dialysed extensively against phosphate buffered saline (PBS), which consisted of 0.14 mol dm^{-3} NaCl, 2.68×10^{-3} mol dm^{-3} KCl, 1.5×10^{-3} mol dm^{-3} KH_2PO_4 and 8.1×10^{-3} mol dm^{-3} Na_2HPO_4, pH 7.5 before use. All solutions used were dialysed to thermodynamic equilibrium with PBS unless otherwise stated.

Solutions for the diffusion cells were made up by the addition of 0.15 mol dm^{-3} of NaCl to the dry material, with compensation for electrolyte exclusion caused by the polyelectrolyte according to the modified Manning theory [20,35]. This facilitated construction of the solutions at the concentration of APM required.

3.2.6. Preparation of low molecular weight [^{3}H]-chondroitin sulfate

50 μl [^{3}H]chondroitin sulfate plus 1 mg unlabelled chondroitin sulfate were dissolved in 1 ml of water within a hydrolysis tube; to this were added 3 ml of 3 M HCl and the tube heated at 70°C in a water bath for 10 min. The tube was then placed on ice and the solution neutralised with NaOH. The solution was then dialysed against PBS and then fractionated on the CPG-120-120 column. Fractions between K_{av} of 0.6

and 0.9 were collected which correspond to dextran molecular weights of 1000 and 5000.

3.2.7. Assays

The concentration of dextran and dextran sulfate was estimated through polarimetry using a Perkin-Elmer 141 Polarimeter (Norwalk, CT). Heparin and chondroitin sulfate were measured by the carbazole method and conversion factors have been described elsewhere [11,37]. Partial specific volumes of the polymers were estimated from density measurements as previously described [9,11,37].

3.2.8. Polynomial analysis

The osmotic and diffusion data were analyzed in terms of a virial expansion by polynomial regression analysis using a curvilinear regression model with orthogonal polynomials on a VAX model 11/780 computer (Digital Equipment Corp.). All osmotic data are based on a temperature of 20 °C.

4. Results and discussion

We can make an approximate estimate of the APM concentration in the GBM through estimates of specific hydraulic conductivity of heparin solutions shown in fig. 2. The hydraulic conductivity decreases markedly with increasing concentration. It is also shown to be independent of the degree of sulfation and of ambient salt concentration. The studies demonstrate that all heparin-like polysaccharides will have similar k values whose magnitude is primarily determined by the nature of the glycosidic linkage [11,37]. If we assume that the single nephron GFR is governed essentially by the heparin-like polysaccharide concentration in the laminae rarae regions of the GBM then an estimate of its concentration can be made from the k data in fig. 2. The volume flux of solvent defining glomerular filtration rate (GFR) as a function of net pressure (ΔP) is

$$J_v = K_f \Delta P \tag{17}$$

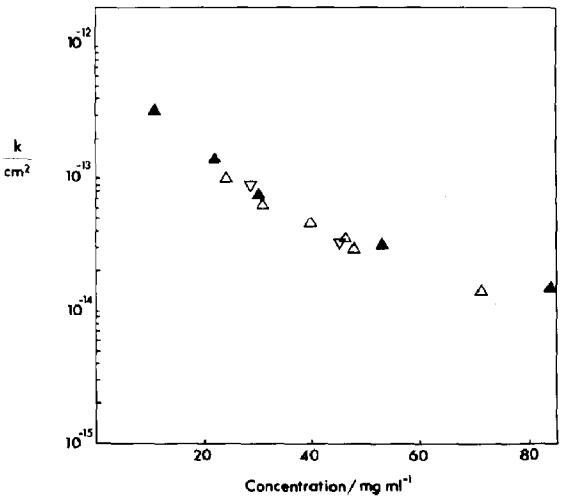

Fig. 2. Variation of the specific hydraulic conductivity k calculated from eq. 5 using data from sedimentation velocity experiments in the analytical ultracentrifuge for heparin in PBS (△) [37] and 1 mol dm^{-3} NaCl (▲), and desulfated heparin in PBS (▽) [11] as a function of concentration.

where

$$K_f = k_2 / A l \eta_3 \tag{18}$$

which is calculated for rat renal flow using K_f the ultrafiltration coefficient for the single nephron, as 0.1 nl/s per mmHg [13,25], A is the effective filtration area which is taken as 10% [12] of the total nephron surface area of 0.0019 cm^2 [18] and l is the thickness which is taken as the sum of the laminae rarae regions which is 100 nm for rat GBM (which is equivalent to two resistance layers each of 50 nm placed in series). Using these figures gives a k of 2.76×10^{-14} cm^2 which corresponds to a heparin-like polysaccharide concentration (from fig. 2) of 40–45 mg ml^{-1}. It is emphasized that this will be an overestimation of GBM APM concentration as no account has been made for the effects of GBM collagen on the GFR. However, it turns out that coincidentally, this APM concentration is similar to the value predicted by Deen et al. [12] when their value of charged concentration in the GBM is converted into heparan sulfate mass concentration (vide supra). Further, it is likely that this APM concentration could not be much higher as rat GBM

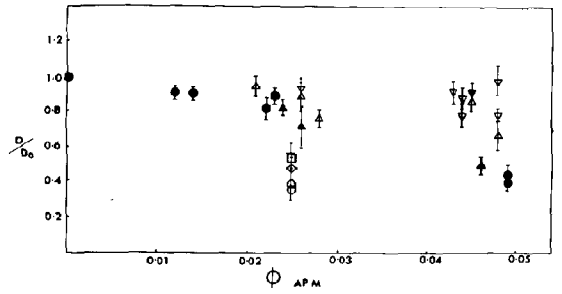

Fig. 3. Variation of the reduced diffusion coefficient $(D/D_0)_1$ (where D_0 is the diffusion coefficient at infinite dilution; table 1) as a function of volume fraction of the APM of dextran test probes, [^{3}H]DEAE dextran (i) (▽) and (ii) (△) (see also table 1), [^{3}H]dextran (●) and [^{3}H]dextran sulfate (▲) in dextran sulfate APMs and of DEAE dextran (i) (○), dextran (◇) and dextran sulfate (□) in chondroitin sulfate APMs. The error bars represent standard errors.

heparan sulfate proteoglycan with a molecular weight of 150000 [17] would be expected to have spherical dimensions of 40–50 nm if fully hydrated. Therefore, regions associated with the laminae rarae would contain heparan sulfate proteoglycan not much more than a single molecule thick.

The diffusional transport of low molecular weight ^{3}H-labelled dextran test probes, namely, DEAE dextran, dextran and dextran sulfate whose physicochemical properties are described in table 1, has been measured as a function of APM concentration afforded by either high molecular weight dextran sulfate or chondroitin sulfate (fig. 3) or the neutral polysaccharide matrix afforded by dextran (fig. 4). The assumption that diffusional transport properly reflects the relative dynamic characteristics of the test probes within the GBM in vivo, where both convectional and diffusional transport are known to occur, is probably not severe as charge selectivity for both types of transport will be governed by the same type of polyion-polyion interaction. For the transport of test probes in dextran sulfate APMs there is a decrease in the reduced diffusion coefficient with increasing volume fraction of the APM. This is a reflection of the frictional interaction of all the test probes with the matrix. Similar reductions have been observed for protein transport in polysaccharide matrices and for concentration-dependent tracer diffusion studies of neutral polymers [23]. The degree of interaction is independent of the molecular weight of the probe as demonstrated by the behaviour of the DEAE dextran probes of different molecular size (fig. 3). Quantitative theoretical predictions of the variation in reduced diffusion coefficient are not available; however, there are some further important qualitative features of these data. At volume fractions less than 0.03 for the various APMs there was no significant difference between the reduced diffusion coefficients of the three charge types of dextran test probes. This would correspond to charge concentrations less than 370 mequiv. l^{-1} for dextran sulfate and 170 mequiv. l^{-1} for chondroitin sulfate. Therefore, at APM concentrations equivalent to, or considerably greater than the predicted APM concentration in the GBM, the electrostatic contribution to dynamic polyion-polyion interaction is negligible. This concurs with the assumption by Deen et al. [12] in their theoretical biophysical treatment of glomerular transport that transport of test probes within the GBM would not show charge selectivity. The lack of any significant electrostatic contribution to polyion-polyion interaction is confirmed by the similar reductions in the diffusion coefficient of the test probes when studied in uncharged dextran polysaccharide matrices (fig. 4).

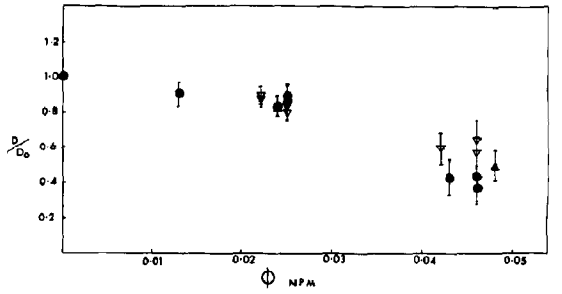

Fig. 4. Variation of the reduced diffusion coefficient for [^{3}H]DEAE dextran (i) (▽), [^{3}H]dextran (●) and [^{3}H]dextran sulfate (▲) in dextran polysaccharide matrices (NPM) as a function of the volume fraction of NPM. The error bars represent standard errors.

Another feature of the data in fig. 3 is that at equivalent APM volume fractions the chondroitin sulfate APM offers considerably more resistance to diffusional transport as compared to the dextran sulfate APMs. This may reflect the different conformation and glycosidic linkage of chondroi-

tin sulfate in exerting higher frictional interaction with the test probes. Yet, no charge selectivity was observed with this APM. It is only at high volume fractions of dextran sulfate APM (i.e., 550 mequiv. l^{-1}) that charge selectivity is detected where DEAE dextran is seen to have a significantly higher reduced diffusion coefficient as compared to the dextran and dextran sulfate probes. The hindrance offered by APM to neutral and negatively charged probes even at high APM values is charge independent, indicating that the electrostatic contribution to dynamic polyanion-polyanion interaction is negligible.

In vivo clearance studies suggest that discrimination of charged solutes relative to dextran of essentially the same hydrodynamic size was greatest for the negatively charged probe dextran sulfate. Maximum selectivity is seen with the relative clearance of dextran sulfate to dextran being in the ratio of 0.04 as compared to that of DEAE dextran to dextran of 4.0 [12]. In using dextran sulfate as a test probe, as well as APM material in the model system, we would expect to amplify the electrostatic contribution to polyion-polyion interaction as the dextran sulfates have considerably higher charge densities than the heparin-like polysaccharides.

Direct experimental measurement of the partitioning of the test dextran probes described in table 1 with 40 mg ml^{-1} dextran sulfate APM (or 220 mequiv. l^{-1}) under physiological conditions by frontal gel chromatography revealed that the partitioning of all the probes was essentially unity. In other words, the 40 mg ml^{-1} dextran sulfate matrix did not exert any significant exclusion of either the entropic or charge interaction kind at this concentration. It is only when the dextran sulfate is studied at relatively high concentration (60 mg ml^{-1}) that we did eventually see a small partition of the dextran sulfate probe (radius = 17 Å, table 1) (fig. 5). The partition coefficient of the [^{3}H]dextran sulfate probe in this APM matrix was 0.88 (obtained from the ratio of the two plateaus of labelled material in fig. 5 ($n = 3$)). The distribution represents the ability of the probe to partition itself between the mobile (extra bead space) phase of the column (where the APM material is retained) and the stationary phase (internal bead

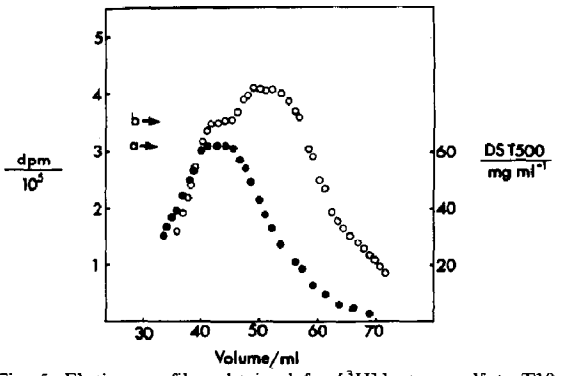

Fig. 5. Elution profiles obtained for [^{3}H]dextran sulfate T10 (○) in frontal gel chromatography of dextran sulfate T500 (DST500) 60 mg ml^{-1} (●) in PBS on a column (1.8 × 52 cm) of controlled-pore glass A240 equilibrated with PBS. The arrows a and b represent the initial concentrations of dextran sulfate T500 and [^{3}H]dextran sulfate T10, respectively. The K_{av} for the [^{3}H]dextran sulfate T10 with controlled-pore glass A240 was greater than 0.95.

space) of the column (which is APM free but is essentially totally accessible to small test probes like [^{3}H]dextran sulfate ($K_{av} > 0.95$)). This value compares with the partitioning of neutral dextran (radius = 20 Å, table 1) of 0.95 for the same dextran sulfate matrix at 60 mg ml^{-1}. These results suggest that polyion-polyion electrostatic interaction contributing to the partition coefficient was small. It is certainly clear that these experimental values do not compare at all with the predictions of the partition coefficient by Deen et al. [12]. For an APM concentration of 330 mequiv. l^{-1} and a dextran sulfate probe of 17 Å in radius a partition coefficient of approx. 0.25 is predicted [12] purely on the grounds of electrostatic interactions. Even at an APM concentration of 160 mequiv. l^{-1} a partition coefficient of 0.65 is estimated on the basis of the model of Deen et al. [12] which is consistently lower than that obtained in the model experimental and theoretical systems studied here. This suggests that equilibrium polyion-polyion interaction exhibited essentially no charge selectivity at the high charge concentration of the APM studied. Additional investigations of chondroitin sulfate APM revealed a similar lack of partitioning. The partitioning of low molecular weight chondroitin sulfate in 40–60 mg ml^{-1}

chondroitin sulfate APMs in PBS was found to be 0.95 or higher.

The lack of experimental confirmation of the predictions of charge selectivity by Deen et al. is also reinforced by theoretical considerations. The Donnan equilibrium considerations (see section 2) would suggest that the partition of the dextran sulfate probe (as a point source) on purely electrostatic grounds, would be inversely proportional to the simple electrolyte distribution (eq. 16) and therefore be greater than unity, whereas polyion-polyion interaction of the excluded volume type would tend to generate a partition coefficient less than unity.

Direct measurement of the electrostatic contribution to polyion-polyion interaction is difficult. However, it is of interest to pursue the problem through an estimate of its magnitude from the analysis of the $(\partial \Pi^*/\partial C)$ data shown in fig. 6 using eq. 12. These studies have been made on two types of APMs, namely, heparin and dextran sulfate. The nonelectrostatic contribution to $(\partial \Pi^*/\partial C)$ for heparin has been estimated by measurements of sedimentation and diffusion in 1 mol dm^{-3} NaCl (table 2). We use the approximation that if the osmotic pressure is purely determined by the Donnan equilibrium then $\Pi^* \propto (1/c_s'')$ [29] so that the osmotic pressure in 1 mol dm^{-3} NaCl will be, at least, 6.66-times lower than that obtained in phosphate-buffered saline (PBS). Using the difference between $(\partial \Pi^*/\partial C)_{PBS}/6.66$ and $(\partial \Pi^*/\partial C)_{1M\ NaCl}$ and reiterating the procedure will give an approximate nonelectrostatic contribution to $(\partial \Pi^*/\partial C)$ (table 3). It is likely that this value will be an underestimate. The nonelectrostatic contribution to $(\partial \Pi^*/\partial C)$ for dextran sulfate in PBS was approximated by the value corresponding to dextran (fig. 6). The results, as shown in table 3, demonstrate that the estimated nonelectrostatic contribution to $(\partial \Pi^*/\partial C)$ is significant, being in the range of 37–53%.

The major feature of these results is that they confirm the experimental partition studies from frontal gel chromatography as described earlier. In terms of the nonelectrostatic contribution to partitioning (table 3) it is only heparin-heparin interaction that may approach the magnitude of in vivo clearance data for the predicted value of Deen et al. (table 3). Dextran sulfate-dextran sulfate interaction would not result in any significant partitioning in nonelectrostatic terms. It seems likely that heparin-dextran sulfate interaction (a model similar to the in vivo interaction) would lie somewhere between the two sets of data.

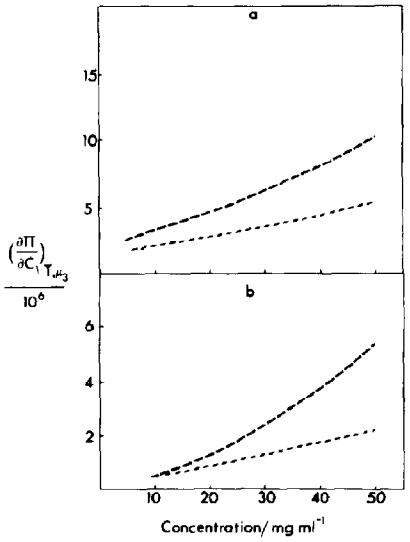

Fig. 6. Variation of $(\partial \Pi^*/\partial C_1)$ obtained from sedimentation-diffusion data using eq. 6 with concentration for (a) heparin in PBS (— — —) (sedimentation/diffusion data from ref. 11) and in 1 mol dm^{-3} NaCl (- - - - -) (table 2) and (b) dextran sulfate in PBS (— — —) [37] and dextran (- - - - -) [9].

Table 2

Hydraulic and diffusion data for heparin in 1 mol dm^{-3} NaCl

	Concentration (mg ml^{-1})	k ($\times 10^{-13}$) (cm^2)	D ($\times 10^{-7}$) ($cm^2\ s^{-1}$)
Specific hydraulic conductivity data	2	20	
	5	7.5	
	11	2.9	
	22	1.2	
	30	0.65	
	53	0.28	
	85	0.13	
Mutual diffusion data	2		6.6
	14		7.2
	26		8.0
	40		8.1

Table 3

Predicted partition coefficients for an anionic test probe of the same chemical composition as the APM (radius 30 Å, molecular weight 15000)

Calculations were performed from the data in fig. 6 through the use of eq. 12 at an APM concentration of 160 mequiv. l^{-1} for dextran sulfate and heparin which is the concentration corresponding to the single nephron k value of 2.7×10^{-14} cm^2. NA, not applicable

APM	Total	$(\partial\Pi^*/\partial C)$		Partition coefficient (K)	
		Electrostatic	Nonelectrostatic	Electrostatic	Nonelectrostatic
Dextran sulfate	3.0	1.4	1.6	1.0	1.0
Heparin	8.0	5.0	3.0	0.143	0.46
Theoretical (Deen et al. [12])	NA	NA	NA	0.023	0.17
In vivo fractional clearance [12]	NA	NA	NA	0.05	0.35

Evaluation of the apparent electrostatic interaction partition coefficient is spurious as it is obtained from the difference $(\partial\Pi^*/\partial C)_{total}$ and $(\partial\Pi^*/\partial C)_{nonelectrostatic}$. Many studies have shown that it is essentially derived from the counterion osmotic activity and salt distribution rather than from the enhancement of electrostatic effects associated with volume exclusion. Therefore, it is likely to represent a gross overestimate of the electrostatic effect on polyion distribution when presented in this manner (table 3). In any case, if the whole $(\partial\Pi^*/\partial C)_{electrostatic}$ was used to describe the electrostatic partition, the values obtained still do not approach that obtained in vivo i.e., 0.05. In the case of the predicted value the heparin-dextran sulfate interaction would lie somewhere between 1.0 and 0.143.

Using the same type of analysis as in table 3, predictions of the partition coefficient associated with systems used in frontal gel chromatography showed marked agreement. No partitioning at all is predicted of dextran sulfate in 40 mg ml^{-1} dextran sulfate (even taking the $(\partial\Pi^*/\partial C)_{total}$ value to estimate K from eq. 12) and for dextran in 60 mg ml^{-1} dextran sulfate APM. The small partitioning of dextran sulfate in 60 mg ml^{-1} dextran sulfate APM may represent the influence on electrostatic effect.

The conclusion from this study is that previous assumptions [12] involving the partition of charged solutes between the GBM and free solution has been shown not to hold and that the biophysical interpretation of charge selectivity cannot explain the quantitative difference observed in vivo. This is consistent with new observations that charge selectivity associated with dextran sulfate clearance has been shown to involve cell-mediated processes [30].

Acknowledgements

This work was supported in part by grants from the National Health and Medical Research Council, the Australian Research Council, Monash University Special Research Grant Fund, the Arthritis Foundation of Australia and the Australian Kidney Foundation. We gratefully acknowledge discussions with Dr J.D. Wells (Bendigo College of Advanced Education) concerning the Donnan equilibrium associated with a permeant polyanion species.

References

1 C.M. Bennet, R.J. Glassock, R.L.S. Chang, W.M. Deen, C.R. Robertson and B.M. Brenner, J. Clin. Invest. 57 (1976) 1287.
2 J. Bray and G.B. Robinson, Kidney Int. 25 (1984) 527.
3 M.P. Bohrer, C. Baylis, H.D. Humes, R.J. Glassock, C.R. Robertson and B.M. Brenner, J. Clin. Invest. 61 (1978) 72.
4 M.P. Bohrer, C. Baylis, C.R. Robertson and B.M. Brenner, J. Clin. Invest. 60 (1977) 152.
5 M.P. Bohrer, W.M. Deen, C.R. Robertson and B.M. Brenner, Am. J. Physiol. 233 (1977) F13.

6 R.L.S. Chang, W.M. Deen, C.R. Robertson and B.M. Brenner, Kidney Int. 8 (1975) 212.
7 R.L.S. Chang, I.F. Ueki, J.L. Troy, W.M. Deen, C.R. Robertson and B.M. Brenner, Biophys. J. 15 (1975) 887.
8 W.D. Comper and T.C. Laurent, Physiol. Rev. 58 (1978) 255.
9 W.D. Comper, B.N. Preston and P. Daivis, J. Phys. Chem. 90 (1986) 128.
10 W.D. Comper and R.P.W. Williams, J. Biol. Chem. 262 (1987) 13464.
11 W.D. Comper and O. Zamparo, Biochem. J. 269 (1990) 561.
12 W.M. Deen, B. Satvat and J.M. Jamieson, Am. J. Physiol. 238 (1980) F126.
13 W.M. Deen, J.L. Troy, C.R. Robertson and B.M. Brenner, J. Clin. Invest. 52 (1973) 1500.
14 H. Fujita, Mathematical theory of sedimentation analysis (Academic Press, New York, 1962).
15 Y.S. Kanwar and M.G. Farquhar, Proc. Natl. Acad. Sci. U.S.A. 76 (1979) 1303.
16 Y.S. Kanwar, and M.G. Farquhar, J. Cell Biol. 81 (1979) 137.
17 Y.S. Kanwar, A. Veis, J.H. Kimura and M.L. Jakubowski, Proc. Natl. Acad. Sci. U.S.A. 81 (1984) 762.
18 H. Kirkman and R.E. Stowall, Anat. Rec. 82 (1942) 373.
19 M. Kurata, Thermodynamics of polymer solutions, Vol. 1, Polymer monographs (Harwood Academic, New York, 1982).
20 G.S. Manning, J. Chem. Phys. 51 (1969) 924.
21 P.F. Mijnlieff and W.J.M. Jaspers, Trans. Faraday Soc. 67 (1971) 1837.
22 G.E. Palade, in: Endothelial cell biology in health and disease, eds N. Simionescu and M. Simionescu (Plenum, New York, 1988) p. 3.
23 B.N. Preston, T.C. Laurent and W.D. Comper, in: Molecular biophysics of the extracellular matrix, eds D.A. Rees and E.R. Morris (Humana Press, NJ, 1984) p. 119.
24 L.J. Rosenzweig and Y.S. Kanwar, Lab. Invest. 47 (1982) 117.
25 V.J. Savin and D.A. Terreros, Kidney Int. 20 (1981) 188.
26 R.G. Spiro and P.S. Mohan, in: Renal basement membrane in health and disease, eds R.G. Price and B.G. Hudson (Academic Press, New York, 1987) p. 11.
27 J.L. Stow, H. Sawada and M.G. Farquhar, Proc. Natl. Acad. Sci. U.S.A. 82 (1985) 3296.
28 L.-O. Sundelöf, Anal. Biochem. 127 (1982) 282.
29 C. Tanford, Physical chemistry of macromolecules (Wiley, New York, 1962).
30 M. Tay, W.D. Comper and A.K. Singh, Am. J. Physiol. (1990) in the press.
31 J.P.G. Urban, A. Maroudas, M.T. Bayliss and J. Dillon, Biorheology 16 (1979) 447.
32 M.-P.I. Van Damme, W.D. Comper and B.N. Preston, J. Chem. Soc., Faraday Trans. I, 78 (1982) 3357.
33 M.-P. Van Damme, W.H. Murphy, W.D. Comper, B.N. Preston and D.J. Winzor, Biophys. Chem. 33 (1989) 115.
34 R. Varoqui and A. Schmitt, Biopolymers 11 (1972) 1119.
35 J.D. Wells, Proc. R. Soc. Lond. B. 183 (1973) 399.
36 M. Wolgast and G. Öjteg, Am. J. Physiol. 254 (1988) F364.
37 O. Zamparo and W.D. Comper, Arch. Biochem. Biophys. 274 (1989) 259.